Theory of t_{2g} electron-gas Rashba interactions

Guru Khalsa,[1,*] Byounghak Lee,[2] and A.H. MacDonald[1,*]

[1]*Department of Physics, University of Texas at Austin, Austin TX 78712, USA*

[2]*Department of Physics, Texas State University, San Marcos, TX 78666, USA*

*email:guru@physics.utexas.edu,macd@physics.utexas.edu

The spin-degeneracy of Bloch bands in a crystal can be lifted[1,2] when spin-orbit (SO) coupling is present and inversion symmetry is absent. In two-dimensional electron systems (2DES) spin-degeneracy is lifted by Rashba interaction[3,4] terms - symmetry invariants that are scalar products of spin and orbital axial vectors. Rashba interactions are symmetry allowed whenever a 2DES is not invariant under reflections through the plane it occupies. In this paper, we use a tight-binding model informed by *ab initio* electronic structure calculations to develop a theory of Rashba splitting in the t_{2g} bands of the two-dimensional electron systems[5–9] formed at cubic perovskite crystal surfaces and interfaces. We find that Rashba splitting in these systems is due to atomic-like on-site SO interactions combined with processes in which t_{2g} electrons change orbital character when they hop between metal sites. These processes are absent in a cubic environment and are due primarily to polar lattice distortions which alter the metal-oxygen-metal bond angle.

Bulk cubic perovskites have chemical formula ABO_3 and the crystal structure illustrated in Figure 1a. The 2DESs in which we are interested are formed from conduction band B-site transition metal d-orbitals. Because the B site, at the cubic cell center, has octahedral coordination[10] with neighboring oxygen atoms, located at the centers of the cubic cell faces, oxygen-metal bonding partially lifts the degeneracy of the d-orbitals, pushing the $e_g = \{x^2 - y^2, 3z^2 - r^2\}$ orbitals up in energy relative to the $t_{2g} = \{yz, zx, xy\}$ orbitals (Figure 1b). In the the simplest model of the bulk electronic structure[11], the bonding networks of the three t_{2g} bands are decoupled; an xy-orbital on one B site, for example, can hop only along the y or x direction through an intermediate p_x or p_y orbital to an xy-orbital on the B site of a neighboring cubic cell. In perovskite 2DESs, the t_{2g} bands are reconstructed[12,13]

into 2D subbands whose detailed form depends on the bulk band parameters[14], the surface or interface confinement mechanism, and the dielectric response of the material. A polar displacement of A and B atoms relative to the oxygen octahedra occurs in response to the confinement electric field; this is the same response that is responsible in some materials (including in particular $SrTiO_3$) for extremely large bulk dielectric constants[12,15]. At the same time atomic-like SO splitting interactions hybridize the three t_{2g} orbitals, which are split in the 2DES by differences in their confinement energies. (For $\langle 001 \rangle$ 2DESs (assumed below) xy orbitals, which have weak bonding along the z-direction, have the lowest confinement energy and therefore higher occupancy than $\{yz, zx\}$ bands.) We explain below how these two effects combine to produce a Rashba interaction.

The Rashba interaction couples an orbital axial vector that is odd under $z \to -z$ to spin, and must therefore arise from hopping process that are odd under inversion in the $x-y$ plane. We therefore begin by considering a single plane (see Figure 1c) of metal atoms and identify the relevant process by using a tight-binding model[16] for $p-d$ hybridization, assigning a hopping amplitude t_{pd} to the process discussed above. Because of the difference in parity between p and d orbitals, t_{pd} changes sign when the hopping direction changes (Figure 2). To leading order in t_{pd} virtual hopping via oxygen sites, the Hamiltonian is diagonal in the t_{2g}-space with eigenenergies:

$$\epsilon_{yz} = 4t_1 - 2t_1 \cos(k_y a) \tag{1}$$

$$\epsilon_{zx} = 4t_1 - 2t_1 \cos(k_x a) \tag{2}$$

$$\epsilon_{xy} = 4t_2 - 2t_2 cos(k_x a) - 2t_2 cos(k_y a) \tag{3}$$

Here $t_{1,2} = t_{pd}^2/\Delta_{pd}$ where Δ_{pd} is the splitting between the oxygen p and metal t_{2g} energy levels and the subscripts acknowledge a symmetry allowed difference, ignored below, between xy and $\{yz, zx\}$ hopping amplitudes in the planar environment. Note that the xy band is twice as wide as the $\{yz, zx\}$ bands and lower in energy at the 2D Γ point. Level repulsion from apical oxygens contributes $2t_1$ to $\epsilon_{yz,zx}$. Because effective metal-to-metal hopping amplitudes in this model are independent of hopping direction, they do not produce Rashba splitting even when combined with on-site SO terms.

Rashba interactions are caused by broken mirror symmetry and in particular by the associated electric field E perpendicular to the 2DES plane. For t_{2g} 2DESs, this field both polarizes the atomic orbitals and induces a polar lattice displacement. These effects open new covalency channels in the metal-oxygen network. In particular there is no hopping in the unperturbed system between a metal zx-orbital and an oxygen x-orbital separated along the y-direction. This is because the x-orbital is even and the zx-orbital odd under reflection in the xy-plane passing through the metal-oxygen bond. When $E \neq 0$, the Hamiltonian is no longer invariant under this reflection and the hopping process is allowed. If, for example, we think about the perturbation as arising from an additional potential $-eEz$, we can write the induced hopping amplitude approximately as $E\gamma_1$, where $\gamma_1 = \langle zx, \vec{R} = 0| - ez|x, \vec{R} = a/2\hat{y}\rangle$ (Figure 2a). At the same time, the electric field will produce forces of opposite sign on metal cations and oxygen anions. The induced polarization will change the metal oxygen bond angle introducing a non-zero $\hat{z}$-component direction cosine n in the bond axis direction. In a 2-center approximation, this change also gives a non-zero amplitude nt_{pd} for zx to x hopping along the y direction. Similar considerations imply an identically induced yz to y hopping amplitude along x. (See Figure 2b). Including these weak effects, which at leading order act only once in the two-step metal-oxygen-metal hopping process, we obtain an additional

effective metal-to-metal hopping amplitude that changes sign with hopping direction and therefore produces a Rashba effect. The (yz, zx, xy)-representation Rashba Hamiltonian is

$$H_E^{t_{2g}} = \begin{pmatrix} 0 & 0 & -2it_R \sin(k_x a) \\ 0 & 0 & -2it_R \sin(k_y a) \\ 2it_R \sin(k_x a) & 2it_R \sin(k_y a) & 0 \end{pmatrix}, \tag{4}$$

where the Rashba interaction strength parameter $t_R = (\gamma_1 t_{pd} E)/\Delta_{pd} + (n t_{pd}^2)/\Delta_{pd}$. When combined with the an atomic-like bulk SO interaction[12,14], described in the Supplementary Information, $H_E^{t_{2g}}$ leads to Rashba splitting in the t_{2g} bands. We remark that broken mirror plane symmetry also introduces other covalent bonding channels, but these do not contribute to the Rashba effect. We note that, a surface metal atom in a BO_2 terminated perovskite is not octahedrally coordinated. This absence of local inversion symmetry and the decrease in level repulsion with neighboring oxygen atoms mixes e_g and t_{2g} orbitals at the surface. When this mixing is strong a more elaborate theory of Rashba SO coupling is required.

In general t_{2g} 2DESs will be spread over many coupled metal layers, and the Rashba Hamiltonian $H_E^{t_{2g}}$ will act within each layer with a layer-dependent coupling constant t_R. For the extreme case of a single-layer t_{2g} 2DES, the xy- band will be pulled below the $\{yz, zx\}$-bands by differential confinement effects. In this case we can derive a simple effective Rashba Hamiltonian which acts within the xy subspace. To do so, we define δ as the energy scale which splits the xy and $\{yz, zx\}$ bands at the Γ point. Allowing virtual transitions to the $\{yz, zx\}$ manifold due to orbital/lattice polarization (H_E), and bulk SO effects (H_{SO}), we find the part of the Hamiltonian linear in electric field is given at small k by,

$$H_R^{xy} = \epsilon_{xy}(\vec{k}) - \alpha\, \vec{\sigma} \cdot (\vec{k} \times \hat{z}) \tag{5}$$

where $\alpha = 4\Delta_{SO} t_R a/(3\delta)$.

To support our theory of the Rashba effect we have carried out an *ab initio* study of a typical t_{2g} 2DES. To simplify the comparison we examined the case of a single $\langle 001 \rangle$ BO_2 plane and studied the influences of z-direction external electric fields and oxygen-metal sublattice relative displacements separately. Because we expect Rashba splitting to be proportional to Δ_{SO} we use the $5d$ transition metal Halfnium (Hf) as the B atom. To minimize the mixing between t_{2g} and e_g bands apical oxygen atoms have been included in our study to maintain octahedral coordination of the metal sites and maximize crystal field splitting. Figure 3a shows the band structure of a Hf perovskite plane with ideal atomic positions in the absence of an applied external electric field when spin-orbit interactions are neglected. At the zone center, the xy band has a lower energy than the $\{yz, zx\}$ bands as expected in t_{2g} 2DESs. The strength of the Rashba hopping processes can be read off the band structure by identifying the avoided crossing which occurs between an xz or yz band and the small mass xy band along a large mass direction in momentum space when an electric field is present. We find that even for an extremely large electric field, $0.1eV/\text{Å}$, the level repulsion (Eqn. 4) at the crossing is very small. Figure 3b shows the band structure changes when SO coupling is included. Note the expected confinement-induced t_{2g} manifold degeneracy lifting at the Γ point. On the scale of this figure the Rashba splitting is too small to be visible. Figure 3c plots the spin splitting, which is largest near the band crossing and reaches a maximum value of $\sim 5meV$, as a function of k, and compares it with the splitting predicted by our theory when the value of t_R is fit to the *ab initio* bands calculated in the absence of spin-orbit coupling (see Supplementary Table I for tight-binding fitting parameters).

Figure 4 reports the corresponding results obtained for the case of a polar lattice displace-

ment. Figure 4a shows the bandstructure for a Hf perovskite plane with a displacement of 0.2 Å. The Hf atom displacement was chosen to emulate the interface atomic configuration. According to previous first principles calculation in $LaTiO_3/SrTiO_3$ interface[17], Ti atoms at the interface are displaced out of the TiO_2 plane by $\approx 4\%$ of the lattice constant. For illustrative purposes we report results for a similar Hf atom displacement of $\sim 5\%$ of a lattice constant.

The yz, xz-xy avoided crossing is now easily visible. After SO coupling is included, a clear Rashba splitting is visible (Figure 4b,c) that is an order of magnitude larger than for the orbital polarization case. Note that our t_{2g} only model underestimates the zx band splitting in both cases, particularly close to the band center. We ascribe this to the proximity of the lower e_g level that is visible in the band plots and neglected in our theory.

Our theory of Rashba interactions in t_{2g} 2DESs is consistent with experimental evidence for strong spin-orbit interactions at interfaces between polar and non-polar perovskites[18–20], for example the $SrTiO_3/LaAlO_3$ interface, and in surface 2DESs induced by the very strong electric fields applied by ionic liquid gates. It also suggests that Rashba interactions will tend to be stronger in materials which are more easily polarized. In this sense $SrTiO_3$ has a potential for relatively strong spin-orbit interactions even though Ti is a 3D material. t_{2g} 2DESs with strong lattice polarizabilities may[12] contain both weakly-confined orbitals responsible for superconductivity and strongly-confined orbitals responsibility for magnetism[21]. If so, our theory implies that magneto-transport properties in these materials will be strongly sensitive to local lattice polarization at the surface or interface. We believe that this work provides a starting point for the interpretation of heretofore unexplained magneto-transport phenomena[22,23].

Methods: The first principles calculations were based on the density functional the-

ory and carried out using the Vienna *Ab Initio* Simulation Package[24]. We used projector-augmented wave pseudopotentials and the generalized gradient approximation exchange-correlation functional of Perdew, Burke and Ernzerhof[25]. The supercell contained a three atom HfO_2 layer with two oxygen atoms located directly above and below the Hf atom. The molecular layers were separated by 20 Å vacuum. The plane-wave energy cutoff was set to 500 eV. We employed a $8 \times 8 \times 2$ k-point sampling to achieve electronic convergence.

[1] Kittel, C. *Quantum Theory of Solids* (Wiley, New York, 1963).

[2] Dresselhaus, G. Spin-orbit coupling effects in zinc blende structures, Phys. Rev. **100**, 580586 (1955).

[3] Bychkov, & Y.A., Rashba, J. Oscillatory effects and the magnetic susceptibility of carriers in inversion layers. J. Phys. C: Solid State **17**, 6039-6045 (1984).

[4] Winkler, R. Spin-Orbit Coupling Effects in Two-Dimensional Electron and Hole Systems, Springer Tracts in Modern Physics **191**, (Springer, Berlin, 2003).

[5] Ohtomo, A., & Hwang, H.Y. A high-mobility electron gas at the LaAlO3/SrTiO3 heterointerface Nature **427**, 423 (2004).

[6] Thiel, S., Hammerl, G., Schmehl, A., Schneider, C.W., & Mannhart, J. Tunable Quasi-Two-Dimensional Electron Gases in Oxide Heterostructures. Science **313**, 1942 (2006).

[7] Ueno, K., Nakamura, S., Shimotani, H. & Ohtomo, A. Electric-field-induced superconductivity in an insulator. Nat. Mater. **7**, 855 (2008).

[8] Ueno, K., Nakamura, S. & Shimotani, H. Discovery of superconductivity in KTaO3 by electrostatic carrier doping. Nature Nanotechnol. **6**, 408 (2011).

[9] Mannhart, J. & Schlom, D.G. Oxide Interfaces An Opportunity for Electronics. Science **327**,

5973 (2010).

[10] Goodenough, J.B. *Localized to Itinerant Electronic Transition in Perovskite Oxides* (Springer, Berlin, 1996).

[11] Mattheiss, L.F. Energy Bands for KNiF3, SrTiO3, KMoO3, and KTaO3. Phys. Rev. B **6**, 4718-4740 (1972).

[12] Khalsa, G. & MacDonald, A.H. Theory of the $SrTiO_3$ surface state two-dimensional electron gas. Phys. Rev. B **86**, 125121 (2012).

[13] Stengel, M. First-Principles Modeling of Electrostatically Doped Perovskite Systems. Phys. Rev. Lett. **106**, 136803 (2011).

[14] Bistritzer, R., Khalsa, G, & MacDonald, A.H. Electronic structure of doped d0 perovskite semiconductors. Phys. Rev. B **83**, 115114 (2011).

[15] Neville, R.C., Hoeneisen, B., & Mead C.A. Permittivity of Strontium Titanate. J. Appl. Phys. **43**, 2124 (1972).

[16] Slater, J.C., & Koster, G.F. Simplified LCAO Method for the Periodic Potential Problem. Phys. Rev. **94**, 14981524 (1954).

[17] Popović, Z.S., Satpathy, S., & Martin, R.M. Origin of the two-dimensional electron gas carrier density at the $LaAlO_3$ on $SrTiO_3$ interface. Phys. Rev. Lett. **101**, 256801 (2008).

[18] Caviglia, A.D. Tunable Rashba Spin-Orbit Interaction at Oxide Interfaces. Phys. Rev. Lett. **104**, 126803 (2010).

[19] Jia, C. & Berakdar, J. Magnetotransport and spin dynamics in an electron gas formed at oxide interfaces. Phys. Rev. B **83**, 045309 (2011).

[20] Fete, A., Gariglio, S., Caviglia, A.D., Triscone, J.M., & Gabay, M. Rashba induced magneto-conductance oscillations in the LaAlO3-SrTiO3 heterostructure. Phys. Rev. B **86**, 201105(R)

(2012).

[21] Michaeli, K., Potter, A.C., & Lee, P.A. Superconducting and Ferromagnetic Phases in SrTiO3/LaAlO3 Oxide Interface Structures: Possibility of Finite Momentum Pairing. Phys. Rev. Lett. **108**, 117003 (2012).

[22] Flekser, E. et al. Magnetotransport effects in polar versus non-polar $SrTiO_3$ based heterostructures. Phys. Rev. B **86**, 121104 (2012).

[23] Joshua, A., Ruhman, J., Pecker, S., Altman, E., & Ilani, S. Unconventional Phase Diagram of Two-Dimensional Electrons at the LaAlO3/SrTiO3 Interface. arXiv:1207.7220.

[24] Kresse, G. & Furthmller, J. Efficiency of ab-initio total energy calculations for metals and semiconductors using a plane-wave basis set. Comput. Mater. Sci. **6**, 15 (1996).

[25] Perdew, J. P., Burke K., & Ernzerhof, M. Generalized Gradient Approximation Made Simple. Phys. Rev. Lett. **77**, 3865 (1996).

Acknowledgements: This work has been supported by the Welch Foundation under grant TBF1473 and by the National Science Foundation under grant DMR-1122603. BL was supported by US AFOSR through contract FA9950-10-1-0133.

Competing Financial Interests Statement The authors declare no competing financial interests.

Author Contributions All authors contributed to developing the theory and preparing the manuscript. G.K and B.L. contributed to the DFT calculations.

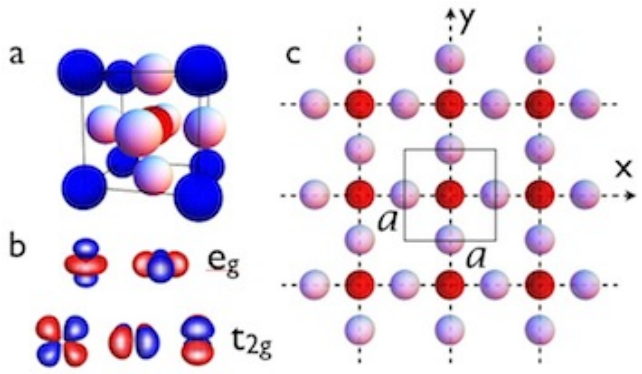

FIG. 1: **Perovskite crystal structure.** **a**, Bulk cubic unit cell with the A atom in blue, B atom in red, and the oxygen in white. **b,** Splitting of atomic d-orbitals into e_g and t_{2g} manifolds. **c,** Single BO_2 plane with one unit cell, with area a^2, in the boxed region.

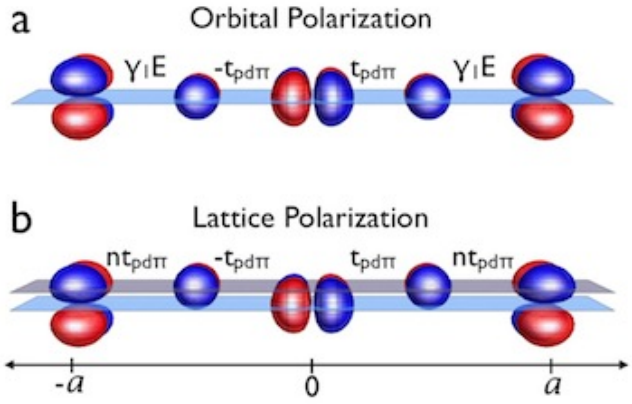

FIG. 2: **Bonding network along the y-axis with an electric field.** **a,** Orbital polarization. Bonding between zx and xy on neighboring metal atoms through p_x orbitals. The positive and negative lobes of the orbital functions are represented in blue and red, respectively. **b,** Lattice Polarization. Displacement of the metal (light blue plane) and oxygen (light purple plane) sublattices in an electric field.

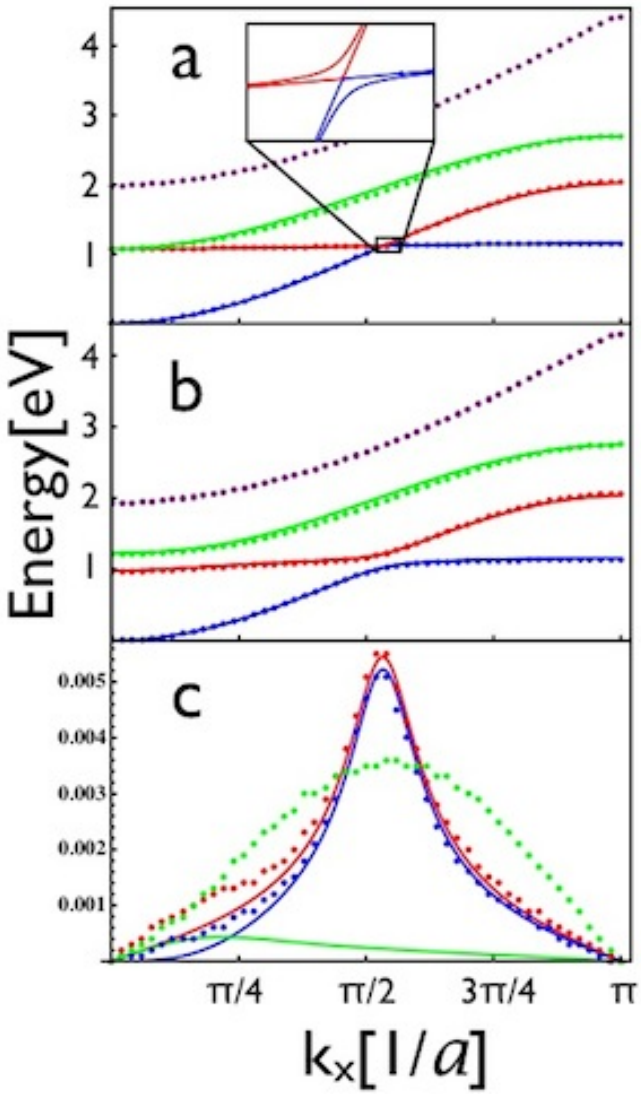

FIG. 3: **Orbital polarization changes to t_{2g} bandstructure.** **a,** t_{2g} bandstructure in the absence of an electric field and SO coupling. The results of our model are shown as solid lines while the simulation is shown as dotted lines. The band order (at the Γ point) is xy (blue), yz (red), zx (green), and $x^2 - y^2$ (purple). The inset shows the onset of an avoided crossing in the presence of an electric field. **b,** t_{2g} band structure with SO coupling and orbital polarization. **c,** Comparison of the orbital polarization part of the Rashba splitting in the t_{2g} space.

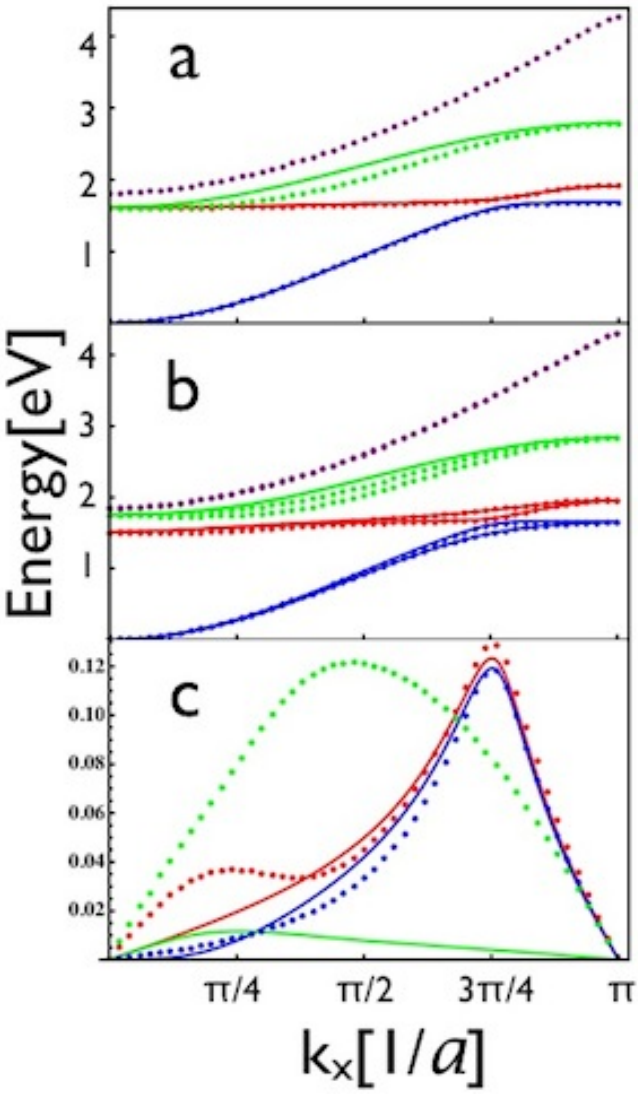

FIG. 4: **Lattice polarization changes to t_{2g} bandstructure. a,** t_{2g} bandstructure in with lattice displacement and no SO coupling. The results of our model are shown as solid lines while the simulation is shown as dotted lines. The band order (at the Γ point) is xy (blue), yz (red), zx (green), and $x^2 - y^2$ (purple). **b,** t_{2g} band structure with SO coupling and lattice displacement. **c,** Comparison of the lattice mediated Rashba splitting in the t_{2g} space.

Supplementary Information

The explicit form of the atomic-like SO coupling Hamiltonian[1,2] mentioned in the main text is given in the $(yz\uparrow, zx\uparrow, xy\uparrow, yz\downarrow, zx\downarrow, xy\downarrow)$ representation by,

$$H^{SO} = \frac{\Delta_{SO}}{3} \begin{pmatrix} 0 & i & 0 & 0 & 0 & -1 \\ -i & 0 & 0 & 0 & 0 & i \\ 0 & 0 & 0 & 1 & -i & 0 \\ 0 & 0 & 1 & 0 & -i & 0 \\ 0 & 0 & i & i & 0 & 0 \\ -1 & -i & 0 & 0 & 0 & 0 \end{pmatrix}. \tag{S1}$$

Breaking the mirror symmetry of the 2DES allows additional covalent bonding terms - not present in the unperturbed cubic system. Those described in the main text are associated with the Rashba effect, but others new processes are allowed. These are summarized in the Table II. In the unpolarized system, the p_x orbital is not involved in the bonding along the x direction. For this reason γ_2 processes, which couples zx and p_x along the x direction, can only contribute to second order in E. The corresponding statement is also true for lattice displacements.

γ_3 increases or decreases the bonding strength with the apical oxygens. If both apical oxygen atoms are present, it can only contribute a term in the Hamiltonian that is quadratic in electric field. At the surface of a BO_2 terminated perovskite, there is a missing apical oxygen. Therefor, within the t_{2g} space and to first order in the electric field, the following term must be added to the Hamiltonian of the surface layer:

$$H_S = \begin{pmatrix} \Delta_S & 0 & 0 \\ 0 & \Delta_S & 0 \\ 0 & 0 & 0 \end{pmatrix}. \tag{S2}$$

In the above equation, $\Delta_S = -E\gamma_3 t_{pd\pi}/\Delta_{pd}$ and may be positive or negative. Because

Tight-Binding Model Parameters		
Lattice Constant	a	4.05 Å
SO splitting	Δ_{SO}	0.340 eV
Orbital Polarization	t_1	0.41 eV
	t_2	0.51 eV
	t_R	0.0014 eV
	t'	0.02 eV
Lattice Polarization	t_1	0.30 eV
	t_2	0.48 eV
	t_R	0.045 eV
	t'	0.02 eV

TABLE I: Tight-binding parameters used in fitting *ab initio* results for HfO_2 plane.

Tight-Binding Matrix Elements		
Lattice Polarization Effects	$\langle xy, \vec{R}=0\vert\Delta U\vert\{x,y,z\}, \vec{R}=\pm\frac{a}{2}\hat{x}+n\frac{a}{2}\hat{z}\rangle$	$\{0,\pm t_{pd\pi},0\}$
	$\langle xy, \vec{R}=0\vert\Delta U\vert\{x,y,z\}, \vec{R}=\pm\frac{a}{2}\hat{y}+n\frac{a}{2}\hat{z}\rangle$	$\{\pm t_{pd\pi},0,0\}$
	$\langle yz, \vec{R}=0\vert\Delta U\vert\{x,y,z\}, \vec{R}=\pm\frac{a}{2}\hat{x}+n\frac{a}{2}\hat{z}\rangle$	$\{0,nt_{pd\pi},0\}$
	$\langle yz, \vec{R}=0\vert\Delta U\vert\{x,y,z\}, \vec{R}=\pm\frac{a}{2}\hat{y}+n\frac{a}{2}\hat{z}\rangle$	$\{0,nt_{pd\pi},0\}$
Orbital Polarization Effects	$\langle xy, \vec{R}=0\vert-ez\vert\{x,y,z\}, \vec{R}=\pm\frac{a}{2}\hat{x}\rangle$	$\{0,0,0\}$
	$\langle xy, \vec{R}=0\vert-ez\vert\{x,y,z\}, \vec{R}=\pm\frac{a}{2}\hat{y}\rangle$	$\{0,0,0\}$
	$\langle yz, \vec{R}=0\vert-ez\vert\{x,y,z\}, \vec{R}=\pm\frac{a}{2}\hat{x}\rangle$	$\{0,\gamma_1,0\}$
	$\langle yz, \vec{R}=0\vert-ez\vert\{x,y,z\}, \vec{R}=\pm\frac{a}{2}\hat{y}\rangle$	$\{0,\gamma_2,0\}$
Apical Oxygen Atoms	$\langle xy, \vec{R}=0\vert-ez\vert\{x,y,z\}, \vec{R}=\pm\frac{a}{2}\hat{z}\rangle$	$\{0,0,0\}$
	$\langle yz, \vec{R}=0\vert-ez\vert\{x,y,z\}, \vec{R}=\pm\frac{a}{2}\hat{z}\rangle$	$\{0,\pm\gamma_3,0\}$

TABLE II: Tight-binding matrix elements for metal t_{2g} and oxygen p-orbitals. The matrix elements for the zx orbitals can be derived from the yz entries, by symmetry.

there is no periodicity in the z- direction, this term is independent of k. In addition, the lack of octahedral coordination at the surface can lead to significant t_{2g}/e_g hybridization.

In addition to the bonding changes to the cubic system mentioned above, if the structural distortions are more complicated (e.g. there is an in-plane twisting of the oxygen octahedra) some σ bonding between the oxygen p and metal t_{2g} orbitals will also be allowed. Provided the polar displacement is still present, these σ bonding channels can also contribute to the Rashba effect.

[1] Khalsa, G. & MacDonald, A.H. Theory of the $SrTiO_3$ surface state two-dimensional electron gas. Phys. Rev. B **86**, 125121 (2012).

[2] Bistritzer, R., Khalsa, G, & MacDonald, A.H. Electronic structure of doped d0 perovskite semiconductors. Phys. Rev. B **83**, 115114 (2011).